CHAPTER 3
PULSED CORONA DISCHARGE FOR ELECTROSTATIC PRECIPITATOR ENHANCMENTS

At present, pulsed corona discharge is a very popular air pollution control. The pulse energization technique has been used to improve the performance of electrostatic precipitator (ESP) and prevent the spark over occurrences between electrodes when used for soot removal. The design and testing of pulse energized ESP was presented in this chapter. The relationships between pulse characteristic and collection efficiency, pulse peak voltage, pulse frequency were investigated. The lab-scale wire-cylinder ESP under the pulse energization was tested and compared to that under a DC-energization. The collection efficiencies at different conditions were also considered.

3.1 Introduction

Soot particulate matters are carbon particles smaller than 10 μm suspended in the atmosphere (David and B. Kittelson 1998,Sagai M. 2001, Takahashi, T. 2000, Yokota H. 2000). For the entrainment, the collection efficiency of soot particles drops sharply when electrical resistivity of particles becomes lower than 10^2 ohm-m (White H.J. 1962). Then, the efficiency cannot increase by increasing voltage due to low electrical resistance of the soot particulate matter. Moreover, with moisture, an electrical breakdown might occur which decrease the efficiency of collecting particle carbon.

This study presented a design and a construction of a pulse-energized ESP for treating soot from an exhaust pipe by using pulse corona discharge technique that generated an electric field between electrodes. The duration of pulse was about ten nanoseconds which was less than the transit time of ion between electrodes. Such pulsed voltage could generate much higher electric fields during pulse without causing spark or electrical breakdown. Therefore, the collection efficiency of ESP could be

increased by increasing the pulse peak voltage between two electrodes that generated the corona discharge current. The parameters affecting the collection efficiency such as pulse duration, pulse frequency, pulse peak voltage and gas flow rate were investigated.

3.2 Theory

The type of ESP used in the present study was a wire-cylinder due to its simple geometry. As shown in Figure 3.1, the volume can be calculated from $\pi L(r_2^2 - r_1^2)$where L is tube length, r_2 is tube radius, r_1 is discharge wire radius, $u_g$and is mean velocity of exhaust gas at inlet. The inner surface area of the outer electrode of the charger is given by $A_c = 2\pi r_2 L$.

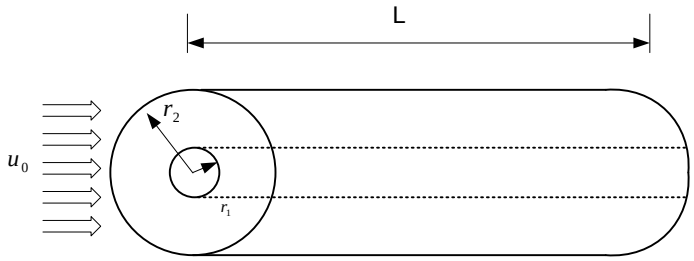

Figure 3.1 The wire-cylinder ESP configurations.

For wire cylinder electrodes, the high voltage power supply connects to the discharge wire electrode while the collecting electrode is grounded. The operating starts up when the supplied voltage is higher than the corona onset voltage to obtain this corona field. The electric field E_c is the field that is required to produce corona, which can be calculated form Equation 2.2 in Section 2.1.2. For wire cylinder electrodes with negative polarity corona and assuming the conductor surface irregularity factor is equal to 1 for smooth and clean conductors, then the E_c can be calculated from

$$E_c = 31\delta\left[1 + \frac{0.308}{\sqrt{\delta r_1}}\right]. \quad (3.1)$$

Where δ is relative air density factor which could be calculated from

$$\delta = \frac{298}{273+t} \cdot \frac{p}{760}. \tag{3.2}$$

Where t is temperature and p is pressure of the ambient air. The corona onset voltage V_c can be calculated from

$$V_c = E_c r_1 \ln\left(\frac{r_2}{r_1}\right). \tag{3.3}$$

The value of corona discharge current starts when the supplied voltage is higher than the corona onset voltage. Then, the whole process of an ESP is mainly depends on the supplied voltage V and current I. The relation for V and I for corona discharge for an ESP defined as

$$\begin{aligned} I &= \frac{8\pi L \varepsilon_0 Z_i}{r_2^2 \ln\left(\frac{r_2}{r_1}\right)} V(V - V_c) \qquad when\ V > V_c, \\ I &\cong 0 \qquad\qquad\qquad\qquad when\ V \leq V_c. \end{aligned} \tag{3.4}$$

The ions concentration between electrodes of ESP is the main cause of particle charging. The particles are charged by the attachment of ions produced by the corona discharge. The ion concentration can be calculated from

$$N_i = \frac{I}{A_c e Z_i E_{ps}}. \tag{3.5}$$

Assuming the obstruction of the flow caused by the wire electrode is neglected due to the very thin wire electrode and the particle velocity is the same to the gas velocity. Therefore, the mean residence time of particles in the charging zone of the wire cylinder ESP can be calculated from

$$t = \frac{\pi r_2^2 L}{Q}. \tag{3.6}$$

As described in Section 2.1.3 (a), the number of diffusion charge (n_{diff}) can be calculated approximately by Equation (2.9), the number field charge (n_{field}) as described in Section 2.1.3 (b) can be calculated by the field charging equation derived by Panthenier and Moreau-Hanot (1932) and White (1951) which is defined in Equation (2.12). Finally, both field and diffusion charging occur at the same time. This is known as continuum charging where the total number of charge on the particle is the sum of the contributions from field and diffusion charging (Liu and Kapadia 1978) as

$$n_p = n_{\text{field}} + n_{\text{diff}} \tag{3.7}$$

$$n_p = \left(1 + 2\frac{\varepsilon-1}{\varepsilon+2}\right)\left(\frac{E_{ps} d_p^2}{4K_E e}\right)\left(\frac{\pi K_E e Z_i N_i t}{1+\pi K_E e Z_i N_i t}\right) + \frac{d_p k_B T}{2K_E e^2} In\left(1 + \frac{\pi K_E d_p \bar{c}_i e^2 N_i t}{2k_B T}\right). \tag{3.8}$$

In field charging, the number of charge on surface area of particle is proportional to the electric filed and square of the particle diameter as shown in the first term of Equation 3.8. Figure 3.2 shows the variation of particle charge number respect to particle diameter with different electric field strength. Equation 3.8 and the parameters in Table 3.1 are used to calculate the number of charges on the particles with the parameters described in the Table. In Figure 3.2, for small enough particle size, the charging mechanism is dominated by ion diffusion and the particle charge number is proportional to diameter in exponential form at various electric field strengths.

Table 3.1 the parameters for calculating the number of charge on surface area of particles

Parameters	Value
Dielectric constant of particle, ε	3
Electric constant, $K_E = 1 / 4\pi\varepsilon_0$	9×10^9
Applied voltage	7 kV, 12kV, 15kV
Discharge wire radius,	0.0015cm
Tube radius,	4.5 cm
Tube length, L	50 cm
Electric field strength ,E_{ps}	1.66 kV/cm, 3.33kV/cm, 6.667 kV/cm
Elementary unit of charge, e	$1.625 \times 10^{-19}C$
Ion mobility, Z_i	$2.2 \times 10^{-4}m^2/Vs$
Boltzmann's constant , k_B	1.380658×10^{-23} J/K
Operating temperature of the system, T	25-300℃
Gas velocity , U_g	0.5 -2m/s
Permittivity of free space,ε_0	8.854×10^{-12} F/m
Mean thermal speed of the ions,$\bar{c}_i$	240 m/s
Particle diameter,d_p	0.1 µm to 10 µm

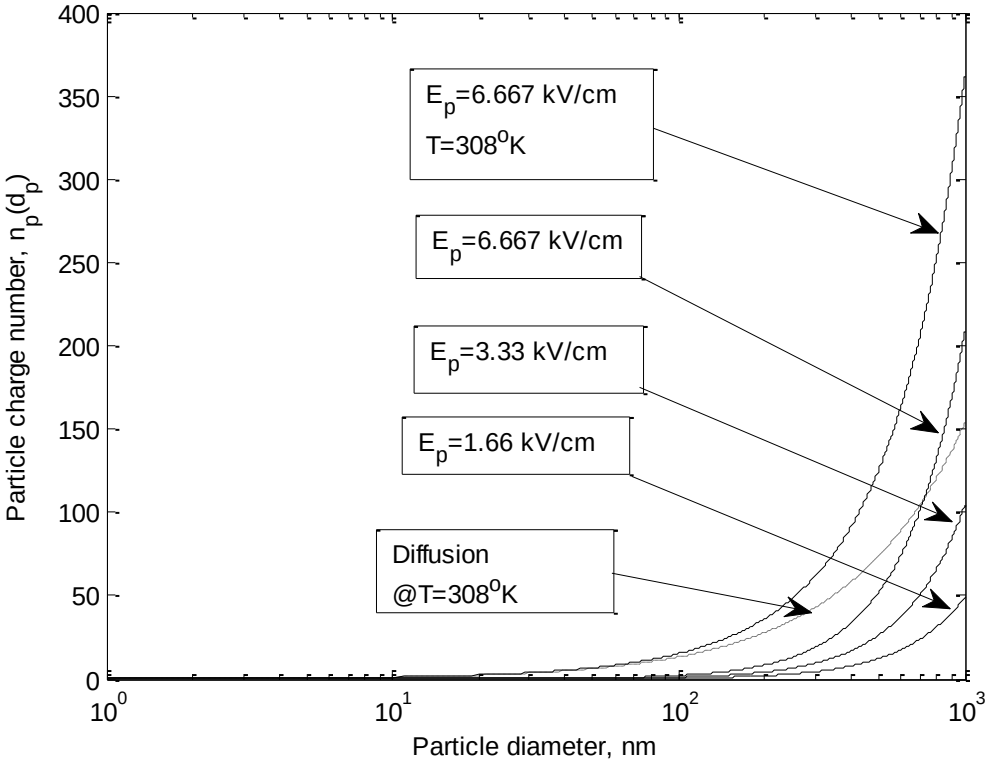

Figure 3.2 The particle charge number on particle size ranged 0.01-1 μm at different electric field strengths.

The mean free path of air is 0.066 μm (Hinds 1999) at 20°C and atmospheric pressure. The mean free path of a certain particle as a function of pressure, P, and temperature, T, is given by

$$\lambda = 0.066 \times 10^{-6} \left(\frac{P_0}{P}\right)\left(\frac{T}{T_0}\right)\left(\frac{1+(115/T_0)}{1+(115/T)}\right). \quad (3.9)$$

The Cunningham slip correction factor C_c can be calculated from

$$C_c = 1 + \frac{\lambda}{d_p}\left(2.34 + 1.05exp\left(-0.39\frac{d_p}{\lambda}\right)\right). \quad (3.10)$$

Viscosity(μ) can be related to a reference viscosity ($\mu_r = 1.81 \times 10^{-5}$ Pa · s) at a reference temperature (T_r =20°C) as the following equation (Willeke and Baron 1993):

$$\mu = \mu_0 \left(\frac{T}{T_0}\right)\left(\frac{1+(115/T_0)}{1+(115/T)}\right). \quad (3.11)$$

With the above equation, n_p is number of charge on the particle calculated from Equation 3.8 , and E_{ce} is electric field strength on the collecting electrode which can be calculated from

$$E_{ce} = \frac{V}{r_2 ln\left(\frac{r_2}{r_1}\right)}. \quad (3.12)$$

The particle migration velocity can be calculated by

$$U_m = \frac{en_p(d_p)}{3\pi\mu d_p} C_c(\lambda) E_{ce}. \quad (3.13)$$

In Figure 3.3, the particle migration velocity calculated by Equation 3.13 with the parameters in Table 3.1,U_m, for fine particles (diameter from 0.1 to 2 μm) is calculated to be about 10 cm/s. This value is much lower than the mean velocity of the gas flow and this is the reason why it is difficult to collect these fine particles. As the particle size increases, the migration velocity becomes larger because the ratio of charge to size increases. However, for particles smaller than 0.1μm the migration velocity increases as the particle size decreases due to the dominant effect of diffusion charging.

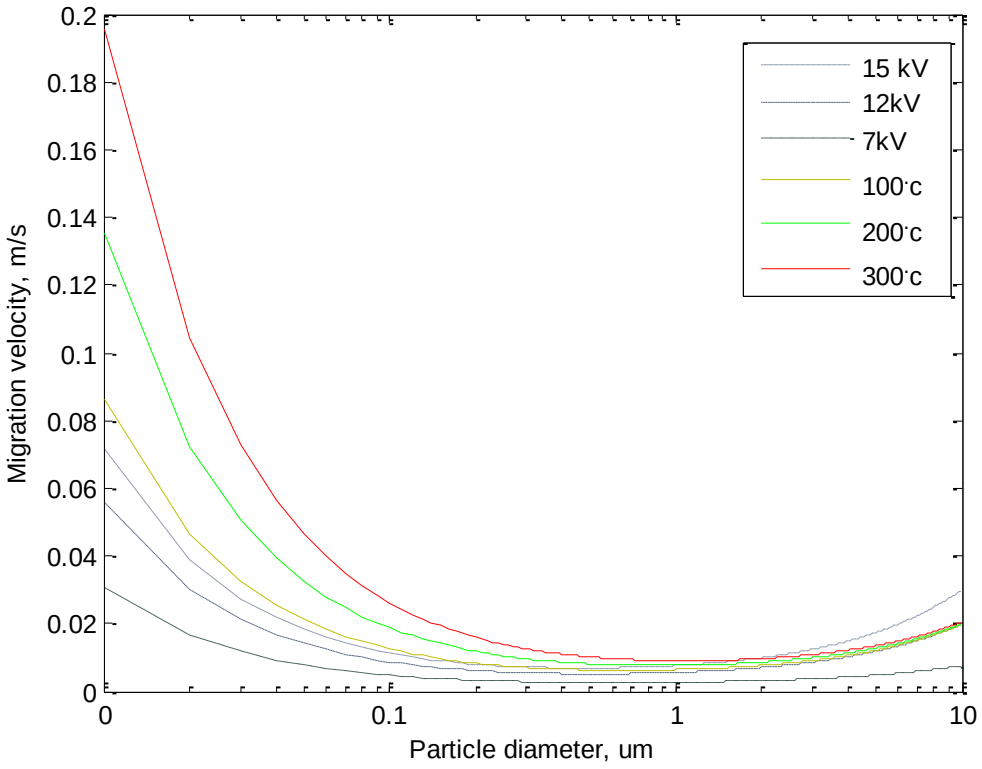

Figure 3.3 The migration velocity of fine particle in wire cylindrical ESP ($r_1 = 0.003cm, r_2 = 4.5cm, L = 50cm, U_g = 0.5m/s$.).

From Figure 3.3, increasing of temperature will increase number of particle charge, as given in Equation 3.8. The number of particle charge describes the amount of ions accumulated in a particle which gives an effect on the migration velocity. As shown in Figure 3.3, the particle migration velocity calculated by Equation 3.13 with the pulse peak voltage,$12\ kV$, for fine particles at gas velocity of 0.5 m/s is changing with gas temperature. Anyhow, it could be noted that the effect of the temperature on the migration velocity is insignificant for the particles having diameter between 0.1 to 1 μm. The results agree with the study of J. D. Bapat (2001) of which the pulse-Energized ESP was performed in a controlled room temperature from normal temperature to about 300 ℃ , shown that the collection efficiency is practically independent of temperature. Therefore, in this study the effect of gas temperature on the ESP performance will be excluded.

In ESP design, the performance model for particle collection inside the precipitator has been suggested by Deutsch. Equation 3.14 shows the total collection efficiency, η_t, normally referred to that of the original Deutsch equation (Equation 2.1) (Equation 2.8) (Equation 2.9) as

$$\eta_t = 1 - \exp(-D_e)\,,\ D_e = U_m \mathrm{SCA},\ \mathrm{SCA} = \frac{A_c}{Q}. \tag{3.14}$$

Where D_e is Deutsch number, SCA is specific collection area, A is effective collecting area, Q is exhaust gas flow rate $= \pi r_2^2 U_g$and U_m is particle migration velocity.

In pulse-energized ESP, pulsed corona discharge produces free electrons. As the electrons flow toward the collection electrode, they encounter particles and particle charging occurs. The residual voltage after pulsed off period is still driving the charge particles toward the collection electrode. According to the above equations, improvement of the total collection efficiency η_t requires high migration velocity as defined in Equation 3.13. High velocity also needs high values of n_p and E_{CE} which depend on the ESP voltage waveform and the breakdown strength of the flue gases. The peak voltage V_p gives the intensity of the corona discharge current *I*, and the residual voltage V_m makes the particles transport between the ESP electrodes. Moreover, a prescribed pulsed high voltage supply that offers appropriate values of both peak voltage, V_p, and residual voltage, V_m, is needed to obtain a highest value for the collecting efficiency. For negative corona, the positive ions in the active zone move back to the discharge wire; whereas the negative ions start to move towards the collecting electrode. The negative ions have mobility $Z_i^- = 2.2 \times \frac{10^{-4} m^2}{Vs}$ (H.J. White 1963), thus a transit time of an ion between the discharge wire, r_1 and the collecting electrode,r_2 at a distance ($r_2 - r_1$) can be calculated from

$$t_d << t_s = \frac{r_2 - r_1}{U_i}. \tag{3.15}$$

Where t_s is a transit time of ions, and v_i is the ion drift velocity as defined as

$$U_i = Z_i^- E. \tag{3.16}$$

The peak voltage duration time(t_d) is must shorter than this time so that the ions will not reach the collecting electrode. Although ion production stops after the peak voltage, the negative ions in the gap will continue to move in the electrical field and form current. The time until the current has completely decayed is close to the ion transit time given in Equation 3.18. After that the next pulse peak voltage can be applied. The time period, t_p, of the pulsed power supply is defined form

$$t_p = t_d + t_s. \tag{3.17}$$

The ions concentration as described by Equation 3.5 can be increased with the discharge current, adjusted by variation of pulse frequency, where f is frequency or pulse repetition rate of the pulse voltage. Because of the pulse-energized ESP was designed for improving precipitation performance and prevent the occurrence of electrical breakdown so that the maximum of pulse frequency must be over ($f \leq \frac{1}{t_p}$).

The above equations are used to evaluate the values for designing an experimental unit.

For our experimental ESP design, an initial collection efficiency of 95% was used. The average gas velocity in the designed ESP was about 1 m/s. The volumetric gas flow rate was 0.003 m^3/s, the temperature of the gas entering the ESP was about 35℃, and the pressure was 1 atm. The designed length for ESP is 0.5 m. Because of economical reason, Bakelite and PVC pipe were used as an electrical insulator between the wire and collection electrodes, as well as the outer chassis of the ESP so that the maximum voltage of 15 kV was used. Details of the design criteria of the ESP are given in Table 3.1.

Table 3.2 Criteria and requirements used in the design of the wire-cylinder ESP

Parameter	Values	Typical values
Air temperature, T(K)	400	Up to 723
Applied voltage negative pulse (kV)	15	10 to 100
Collection efficiency (%)	95	95 to 99.9
Gas velocity u_g(m/s)	1	0.3 to 3
Pressure (atm)	1 atm	$8x10^4$ to $3x10^5$ Pa

The value was selected to be near 95% in order to provide a round number for the dimensions, which were 100 mm outer and 90 mm inner diameter of stainless tube, the discharge wire was tungsten wire with 0.3mm diameter. This value provide the corona onset voltage as 3.5 kV and distance between electrodes is $r_2 - r_1 \approx r_2 = 45\ mm$, that results in drift velocity of 73 m/s in field of 333 kV/m. The typical transit time is 613.66 μs. The peak duration time was $10\ \mu s$ which provided a maximum frequency of 1.4 kHz. The experimental ESP was tested under testing condition in Table 3.3.

Table 3.3 Testing conditions of the designed ESP

Parameter	Value
Diameter of discharge wire, (mm)	0.3
Diameter of tube (mm)	90
Length of tube (mm)	500
Air temperature, T(K)	308
Applied voltage negative pulse (kV)	0-15
Particle diameterd_p(micron)	0.1-100
Gas velocity u_g(m/s)	0.5,1,1.5,2
Pulse duration(μs)	10
Pulse frequency (kHz)	1,20,40, 60

3.3 The Experimental Setup

The experimental setup has been used to observe the collection efficiency of the designed ESP, under DC and pulse energization as shown in Figure 3.4. The experimental setup consisted of a soot generator, an ESP, and a sampling apparatus. Soot generator from diesel burner. A gas flow velocity was controlled by adjust speed of 3 phase motor drive blower. The velocity and temperature of gas were measured with hot wire anemometer DIGICAN DA-44.The sampling of gas for particle measurements was made using a probe with dimensions and sample flow resulting in near isokinetic conditions.

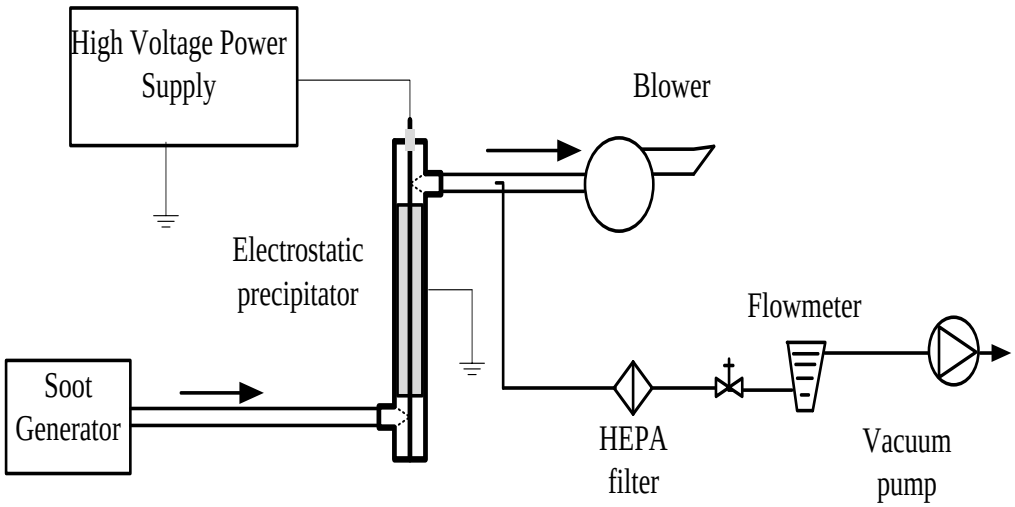

Figure 3.4 Schematic diagrams of the experimental setup.

Figure 3.5 and Figure 3.6 shows a diagram and photo of the wire cylindrical ESP designed and evaluated for this work. A stainless steel pipe was used as a collection electrode. It had a 500 mm length with a 90 mm inside diameter. The discharge electrode was made of tungsten wire with 0.3 mm diameter and 500 mm effective length. The distance between is discharge wire and collecting electrode was 45 mm.

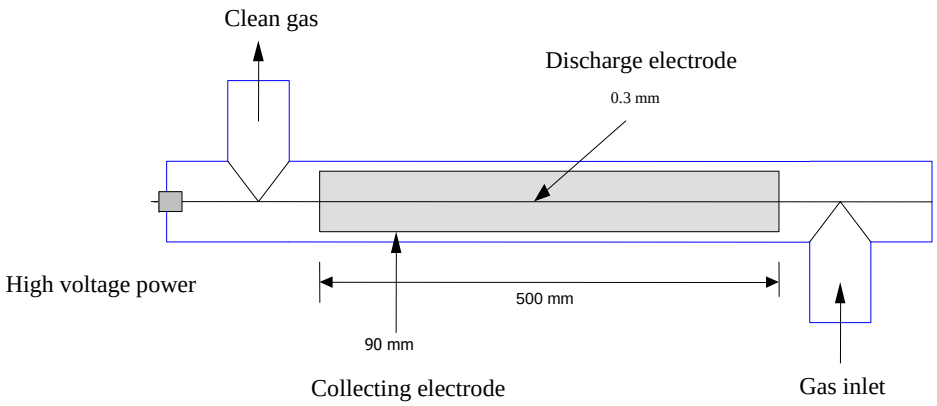

Figure 3.5 The dimensions of the experimental ESP.

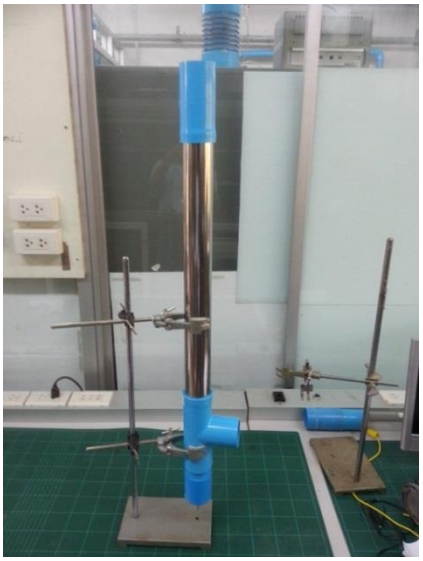

Figure 3.6 Photograph of the experimental ESP.

The pulsed power supply produced high voltage pulse according to the principle of resonant charging. The circuit diagram of the pulse power supply was shown in Figure. 3.7. The DC voltage 12 V from battery was stepped up to 15 kV by a pulse transformer with frequency range around 1 to 60 kHz. Rise time and pulse wide were 400 ns, and 10 μs, respectively. Then, the high voltage AC from the pulse transformer was rectified to be DC pulse by a high voltage diode before supplying to the ESP. The design of pulse power supply shows detail in an appendix A.

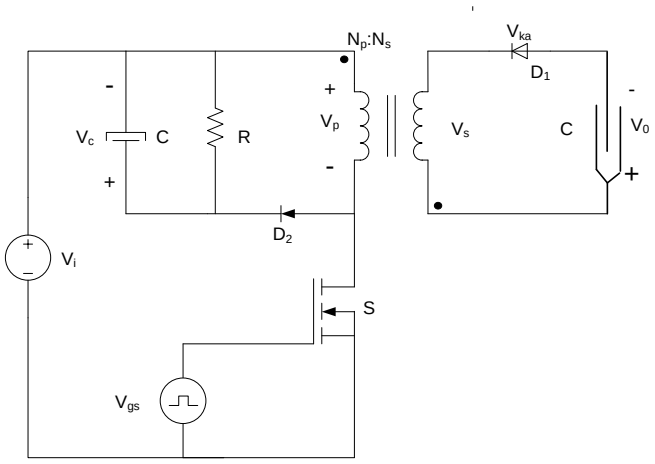

Figure 3.7 The circuit diagram of the pulse power supply.

The average current flow to the ESP was measured by a True-RMS Digital Multi-meters (FLUKE 289) as shown in Figure 3.8, to measure voltage between the collecting electrode and ground. Both the average and peak voltages across the electrode gap were measured with a high voltage probe (FLUKE model 80K-40) as shown in Figure 3.9.

Figure 3.8 True-RMS Digital Multi-meters (FLUKE 289).

Figure 3.9 High voltage probe (Fluke model 80K-40).

The collection efficiency with the mass basis of the ESP was measured for one-hour operation of the soot generator by a high efficiency particulate-free air (HEPA) filter glass fiber of diameter 47 mm as shown in Figure 3.10. The soot was sampled downstream of the ESP every 10 min for 50 min operation. The flow rate was set to be 10 L/min by a modulating valve. A flow meter was used to measure the flow rate which was sucked out by a vacuum pump. The flow meter and the vacuum pump were shown in Figure 3.11 and Figure 3.12, respectively.

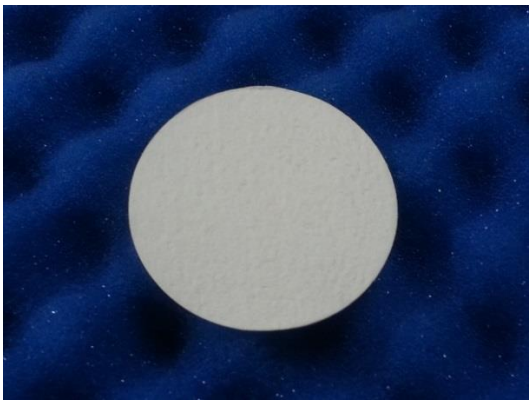

Figure 3.10 High efficiency particulate-free air filter.

Figure 3.11 A gas flow meter.

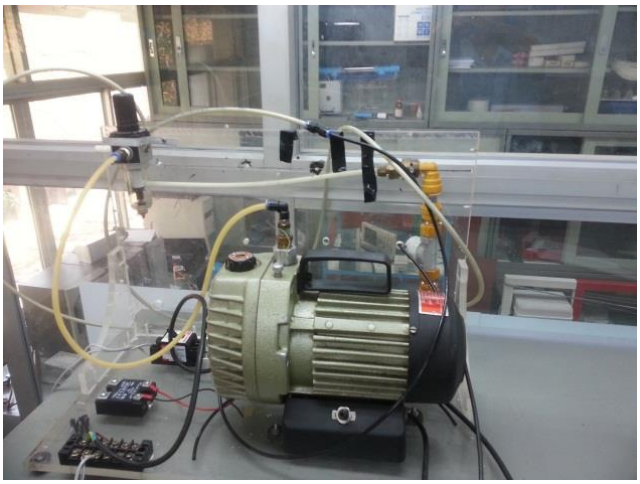

Figure 3.12 A vacuum pump.

The filters were treated prior to use by placing in the desiccator at room temperature with 50-60 % of relative humidity using a sodium dichromate solution as the controller for at least 24 hours before and after the sampling. The filters were then weighted using Digital Weighter Mettler Toledo model PB3002 as shown in Figure 3.13. The first sampling was performed 10 minutes after starting the soot generator.

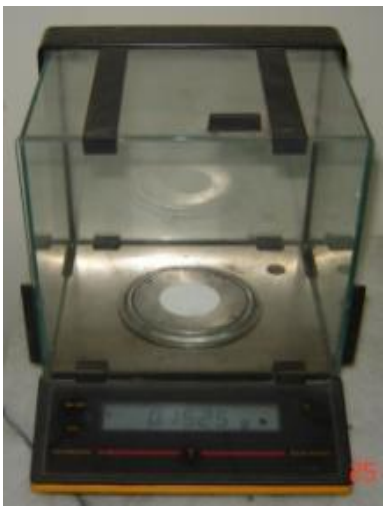

Figure 3.13 A Digital Weighter Mettler Toledo model PB3002.

The weight of collected particles on the filter was measured every 10 min of 1 hour operation using Digital Weighter Mettler Toledo model PB3002. The collection efficiency was plotted as a function of peak voltage. The overall collection efficiency, based on total concentration (all sizes of particles) evaluated from the mass difference on the HEPA filters upstream and downstream of the ESP can be defined by

$$\eta_t = 1 - \frac{M_{out}}{M_{in}}. \qquad (3.18)$$

Where M_{in} and M_{out} are the total masses of all particle sizes at the upstream and the downstream of the ESP channel, respectively. Anyhow, m1 could be directly recorded by the filter downstream when there is no power supply at the ESP.

To measure the number of particles in the exhaust gas, the gas has to be diluted by mixing with clean air and then the mixed gas is sent to the Laser Particle Counter (LPC)P. Figure 3.14 shows the LPC ParticleScan™ CR which is able to measure the number density of particles having sizes between 0.3 to 5 µm at flow rate 0.1 cfm. The fractional collection efficiency, η_f, based on number concentration (0.3 to 5 µm sizes of particles), is evaluated from the number concentrations at the upstream and the downstream of the ESP defined as

$$\eta_f(d_p) = 1 - \frac{N_{out}(d_p)}{N_{in}(d_p)} \quad . \tag{3.19}$$

Where $N_{in}(d_p)$ and $N_{out}(d_p)$ are the number concentrations for a particle size d_p of the particles at the downstream of the ESP, respectively. Again, in practice, $N_{in}(d_p)$ could be monitored downstream when there is no power supply at the ESP.

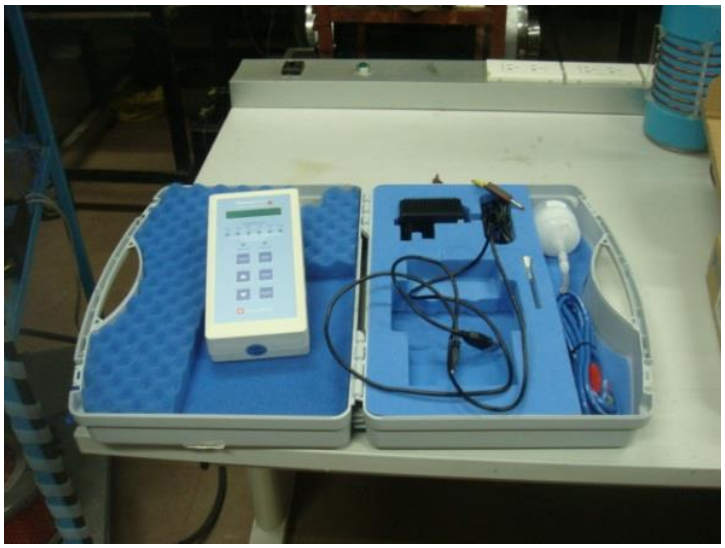

Figure 3.14 Photograph of the particle counter (ParticleScan™ CR).

3.4 Results

3.4.1 Voltage-current characteristics

In this section, the voltage-current characteristics under dust free condition were tested. It also shows that the time average discharge current was increased with the applied voltage. Where the V_o is the onset corona voltage, may give an experimental onset voltage that is variable and much lower than that given by the peek's law. The V-I characteristic of the ESP is shown in Figure 3.16. For supplying high negative voltage, A DC power supply was used, the corona occurred on set voltage 3.2 kV and the current gradually increased with quadratic function of voltage. When supplying voltage was higher than 7 kV, the spark took place between the tungsten wire and the inside cylindrical tube of the electrostatic precipitator. However, when the power supply was replaced by the prototype of high voltage pulse

power supply as shown in Figure 3.15, although the current gradually increased with quadratic function of voltage as same as energized negative DC supply, and increased with increasing pulse frequency. The inception voltage of the corona discharged on the tungsten wire began at 4.5 kV. Nevertheless, the pulse peak voltage can rise up to be higher than spark over voltage of DC-energized. But depended on pulse frequency as shown in Figure 3.14 the spark over voltages were 8 kV, 10 kV, and 12 kV when the pulse frequencies were 40 kHz, 20 kHz, and 1kHzrespectively. But at the pulse frequency low to 1 kHz, the pulse peak voltage could rise up more than 15 kV without spark.

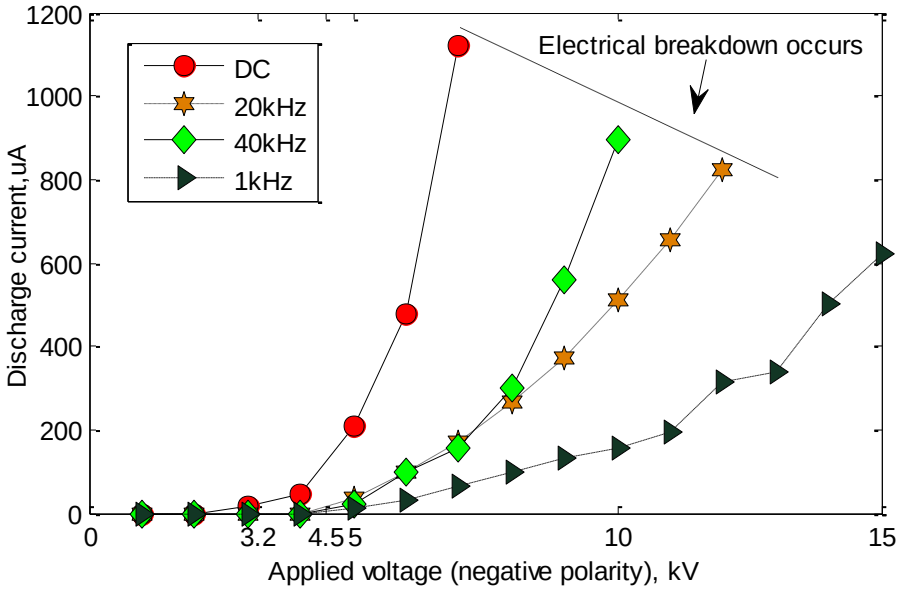

Figure 3.15 Voltage-current characteristics of the designed ESP for DC-energized and pulsed-energized.

In the previous paper, the influence of pulse length which has been varied in the range from 10μs to 1ms with almost rectangular pulse shapes (Egli w. et al. 1997). As a result of the increase in the pulse length by a factor 100, they find an increase of the average current density by only a factor of three. The average current is therefore not very sensitive to pulse length in the tasted.

3.4.2 Collection efficiency of the ESP

The overall collection efficiency for the ESP as a function of both DC and pulse voltage conditions was shown in Figure 3.16. The results indicate that overall collection efficiency was effective higher than 50% when the corona discharges occurred on the tungsten wire in the ESP. The overall collection efficiency was increased while the voltage was increased. Because the electric force on the soot particles was increased by increasing electric field intensity, the collecting carbon particles from exhaust gases also increased. Unfortunately, the high negative voltage must not exceed 7 kV before the breakdown in the DC condition. However, the pulse voltage conditions can increase to10kV without spark. Consequently, the total collection efficiency can be increased up to 74% and 92% by increasing the pulse frequency up to 20 kHz and 40 kHz, respectively. But at The pulse frequency low to 1 kHz, the collection efficiency still lower than 50%.

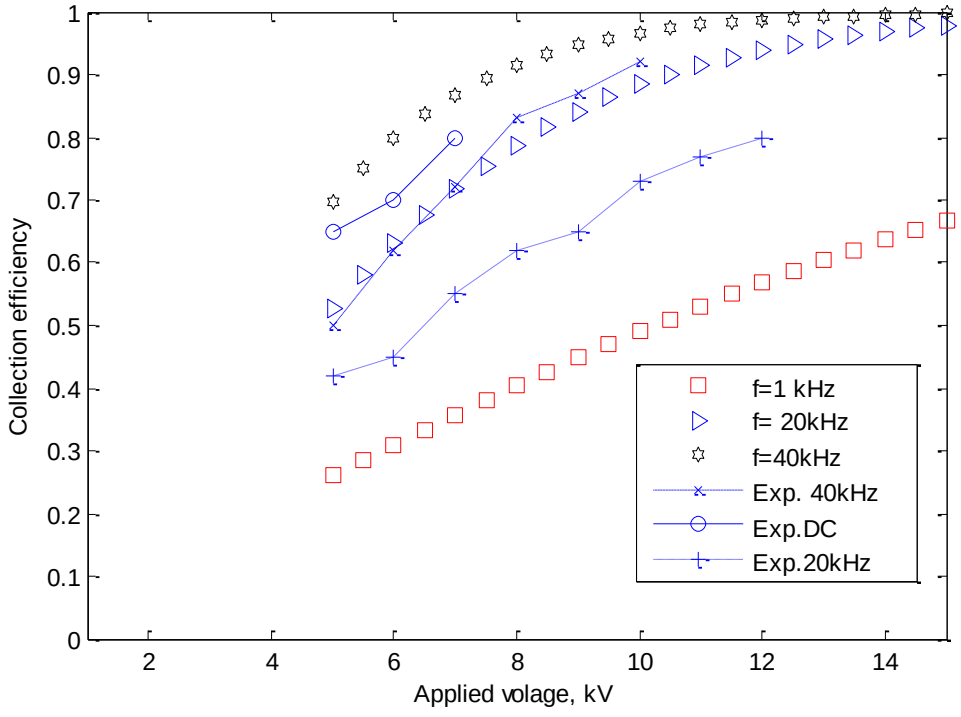

Figure3.16 Variation of the collection efficiency respect to pulse peak voltage with pulse frequency at gas velocity = 0.5 m/s.

3.4.3 Effects of pulse frequency on fractional collection efficiency

Experiments were carried out to investigate the pulse frequency on the fine particle collection efficiency. The gas velocity was controlled at about 0.5 m/s to provide residual time of 1 s in the wire cylinder ESP. A Laser Particle Counter was employed to measure the particle number concentration distributions. The number distributions and their accumulative distributions are shown in Figure 3.17. The measured size fraction ranged from 0.3 μm to 2 μm, which the total number concentration was about 5×10^5 particles/cm^{3}and pulse peak voltage constant at -10 kV is lower than spark-over limit when pulse frequency lower than 60kHz, which provide the best particle charging. Results are represented in Figure 3.18.As shown in Figure 3.19, the pulse frequency was found to play an important role in particle charging. The average number of charges per particle increases rapidly with the increase of pulse frequency. The larger the impulse frequency is, the more energy is produced in the electric field in unit time, which results in higher particle charging. The maximum particle charging effect was obtained at pulse frequency of 40 kHz.

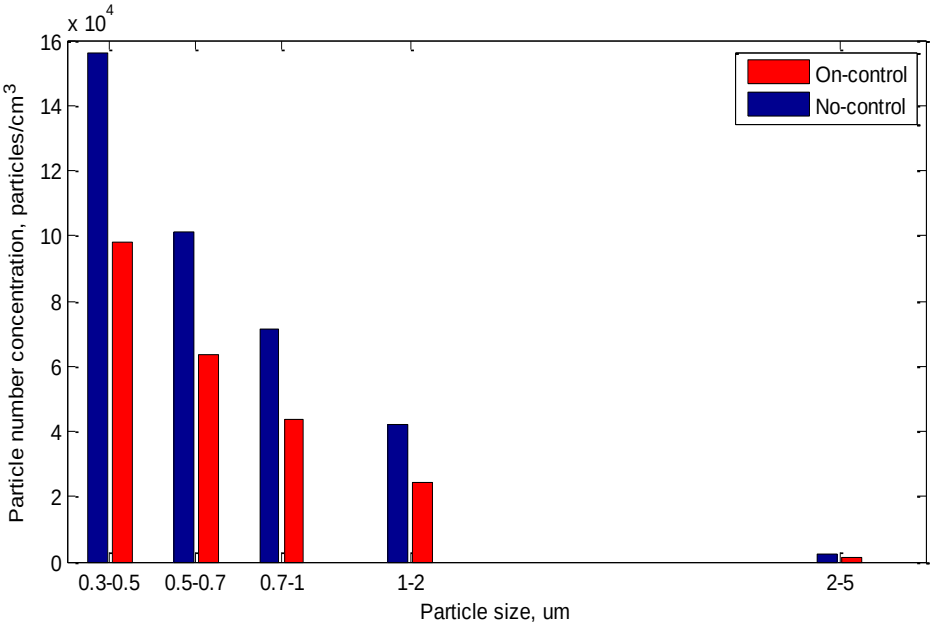

Figure 3.17 The size distribution of aerosol particle downstream of ESP operated at negative pulse voltage 10kV. The particle number concentration was measured at downstream of ESP with (On-control) and without the power supply (No-control), respectively. When the gas velocity was 0.5m/s.

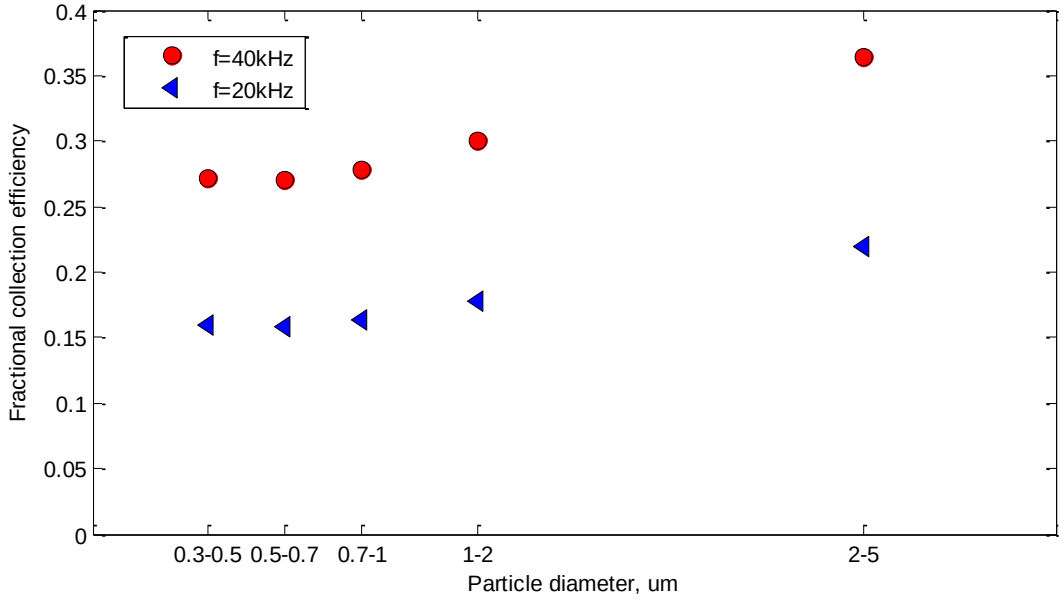

Figure 3.18 Variation of the fractional collection efficiency respect to respect to particles size (difference size rang 0.3µm, 0.5µm, 0.7µm, 1µm, 2 µm) for various pulse frequency when the negative pulse peak voltage, V_p=10kV, the particle number concentration, N =5×10^5 particles/cm^3, the gas velocity u_g=0.5m/s.

Effects of gas flow rate on fractional collection efficiency as shown Figure 3.1 9 present the fractional collection efficiency as a function of gas velocity in the ESP. Experiments were performed by setting the applied pulse peak voltage and pulse frequency constant at 10 kV and 40kHz, respectively. The dust loading was controlled at about 5×10^5 particles/cm^3.The gas velocity was adjusted from 0.5 m/s to 2 m/s to provide gas residence time of 1 s to 0.25 s in the ESP. As shown in Figure. 3.19, it was found that the fractional collection efficiency of particles size 0.3 µm, 0.5 µm, 0.7 µm, 1 µm, 2 µm increases as the residence time increases until 0.5 s, that the particle charging amount increase more than, which means, the diffused charging have been dominant in situation.

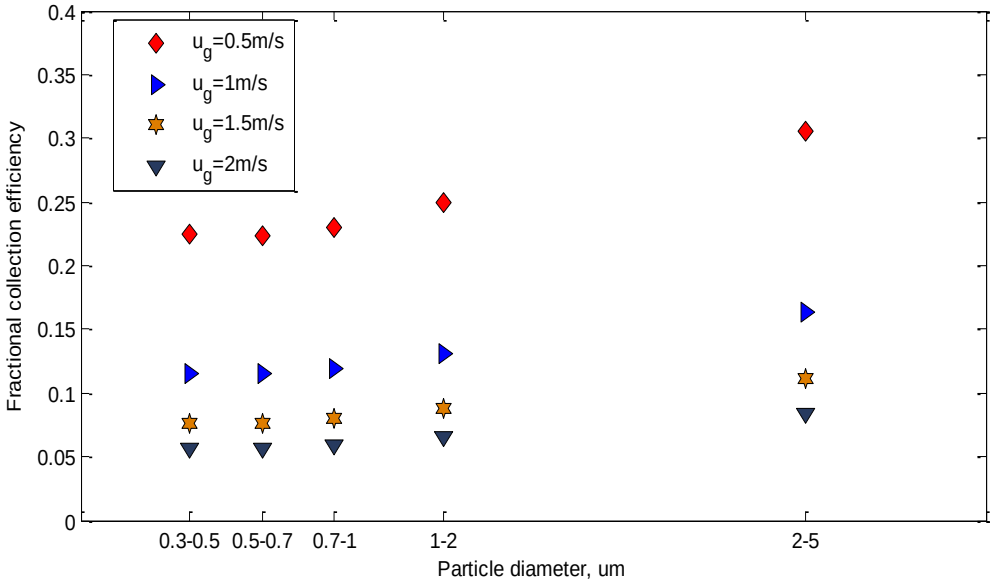

Figure 3.19 Variation of the fractional collection efficiency with respect to particles size (difference size rang 0.3µm, 0.5µm, 0.7µm, 1µm, 2 µm) for various gas velocity when the negative pulse peak voltage, V_p=10kV, The particle number concentration, N $=5 \times 10^5$ particles/cm^3, pulse frequency, f = 40 kHz.

Experiments were carried out to investigate the pulse peak voltage on the fine particle collection efficiency. The gas velocity was control at about 0.5 m/s to provide residual time of 1 s in the wire cylinder ESP. The particle size ranged from 0.3 µm to 2 µm, which the total number concentration was about 5×10^5 particles/cm^3.To avoid break down completely, both the negative pulse peak voltage and pulse frequency would have to be controlled, the negative pulse peak was adjusted from 7 kV, 10 kV, and 12 kV while the pulse frequency constant at 20 kHz. Results are represented in Figure 3.20. As shown in Figure3.21, the pulse peak voltage was found to play an important role in particle charging and particle migration velocity. The collection efficiency for particle size 2 µm increases rapidly with the increasing of pulse peak voltage but small gain for the particle smaller than 1 µm.

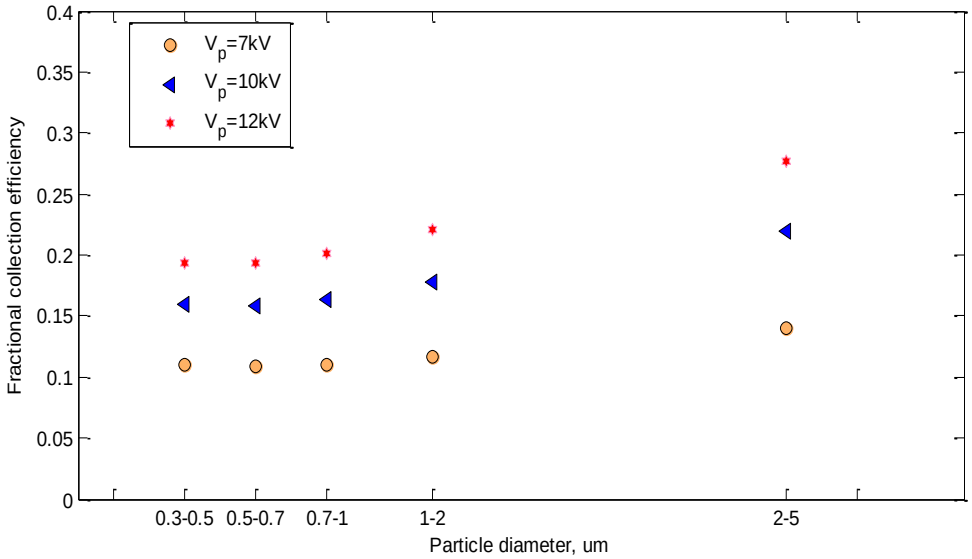

Figure 3.20 Variation the fractional collection efficiency with respect to particles size(difference size rang 0.3µm, 0.5µm, 0.7µm, 1µm, 2µm) for various pulse peak voltage when pulse frequency, f= 20kHz, particle number concentration, N =5×10^5 particles/cm^3, gas velocity, u_g=0.5m/s.

3.5 Conclusion

Voltage pulses faster than the ion transit time from discharge wire to collecting electrode have been applied and effect of slow ion movement has been used to in wire cylinder ESP. In pulse-energized, the pulse peak voltage can be set much higher than the sparking limit at DC-energized. We have described the design and construction of the electrostatic precipitator (ESP) for carbon particle from soot generator. The high voltage power supply has applied high voltage pulse energizing to excite the electric field between electrodes. Moreover, the comparisons of the field exciting between the high voltage pulses energizing and high voltage direct current energizing had been studied. In general, it was found that high voltage pulse energizing not only used lower energy but also had higher efficiency than the DC condition. In pulse condition under the same configuration of the ESP, because the electrons between electrodes have energized into the high energy without spark over in the electrode gap, the total collection efficiency can be increased up to 98% at -10kV at the pulse frequency was 40 kHz.